Advancements in MXenes

Vishal Chaudhary, Akash Sharma, Pradeep Bhadola, and Ajeet Kaushik

Abstract MXenes have gained an excessive interest in architecting new-generation wearable devices owing to their unique physicochemical characteristics and machine processability. Accordingly, different strategies for scalable manufacturing of MXenes are explored for its mass-level production. Using a large reactor with optimal control of reaction parameters, the chemical etching approach has emerged as a feasible, scalable strategy to synthesize MXenes. Moreover, alternative precursors like non-MAX phases and 'i-MAX' phases have advanced these synthesis strategies with a new prospect of scalable production. These developments have projected MXene as a promising candidate to design next-generation wearable electronics with advanced features like intelligent operation, portable, compact, self-powered, flexible, stretchable, bendable, and skin embedded nature. Due to these features, MXenes and their hybrids with materials such as macromolecules, graphene-based materials, and metals are the current choice of advanced nanomaterials to fabricate wearable physical, chemical, and biosensors with excellent performances. These materials have consistently excellent sensing performance in all wear and tear situations and possess biomedical, agriculture, workplace safety, and environmental monitoring applications. Besides excellent electric conductivity and the prospect of accommodating skin depth factors, MXene based materials are used to design wireless communication systems supporting Bluetooth, WiFi, and 5G requirements. It anticipates the

V. Chaudhary (✉)
Research Cell and Department of Physics, Bhagini Nivedita College, University of Delhi, New Delhi 110075, India
e-mail: chaudhary00vishal@gmail.com; drvishal@bn.du.ac.in

A. Sharma
School of Biological and Environmental Sciences, Shoolini University, Solan, Himachal Pradesh 173212, India

P. Bhadola
Centre for Theoretical Physics and Natural Philosophy, Nakhonsawan Studiorum for Advanced Studies, Mahidol University, Nakhonsawan 60130, Thailand

A. Kaushik
NanoBioTech Laboratory, Health System Engineering, Department of Environmental Engineering, Florida Polytechnic University, Lakeland, FL 33805, USA

M. Khalid et al. (eds.), *Fundamental Aspects and Perspectives of MXenes*, Engineering Materials, https://doi.org/10.1007/978-3-031-05006-0_12

enormous potential of MXene based materials to architect field-deployable compact sensors for personalized healthcare monitoring with intelligent wireless operation.

Keywords Wearable electronics · MXene · Wireless communication · Scalable production · Sensors

1 Advancement in Scalable Fabrication of MXenes

MXenes is a large class of 2-D metal carbides and nitrides showing tremendous potential to address diversified global challenges, including water scarcity, energy crisis, environmental redemption, and human health [1–3]. Unlike other 2-D materials, MXenes are generally hydrophilic with abundant surface functionalities with tunable capacity [1]. The desired application area can be easily targeted by optimizing these functionalities and tuning interlayer distance [4]. It has led to extensive dedicated research to find efficient fabrication strategies for high yield MXenes with the desired structural and chemical configuration. Many in-lab experimental strategies to architect MXenes have already been reported, including selective etching, exfoliation, chemical vapor deposition, atomic layer deposition, and green routes [1–3]. Due to low yield, high cost, and sophisticated instrumental requirements, these strategies are constrained for practical purposes [2, 3]. The main challenge associated with MXene mass-production is maintaining its excellent conductivity with mechanical strength simultaneously during machine processing. The bottom-up strategies, such as CVD or ALD, are limited due to issues relating to the requirement of using vacuum chambers and substrates for growth-limiting the final size of MXene [2, 5, 6]. However, these constraints are not present in top-down approaches.

Nevertheless, specific conditions required to be maintained in large reaction volumes are challenging [5]. It restricts the transfer of MXene technology from laboratories to industries, which indicates the need for scalable production. Nevertheless, MXenes do not possess any inherent limitation for synthesis batch size, and the scaling of MXene possibly is theoretically possible without any upper limit [5, 7]. The immediate attention to scalable production of MXenes is dedicated to tuning reaction parameters to optimize desired requirements.

1.1 Issues Related to Scalable Production

Controlling the size of reactor and uniform mixing simultaneously

The scaling of chemical reaction parameters is challenging due to critical factors such as technological and safety issues. For instance, to scale a reactor, non-linear effects like the surface-to-volume ratio of the reactor must be considered. In addition, the transfer of two reactants creates a significant issue when adding the desired relative quantities of precursors [5, 8, 9]. It indicates the importance of continuous uniform

stirring or mixing of precursors during the course of a reaction. Hence, the prime aspect of MXene machine processing is designing uniform mixing larger reactors. However, optimizing mixing parameters during the reaction in such a larger reactor is challenging and yet to be established.

Controlling heat transfer during reactions

There is a drastic change in heat transfer from the fluid to the reactor due to less relative reactor surface area available for cooling [5, 10]. It raises the concern of initiating runaway reactions and anticipates explosion. Hence, it results in an alteration in the reactor's internal temperature during production. It can affect the chemical kinetics of reactions and properties of the resultant product. Moreover, it can adversely affect the lattice arrangement, surface functionalities, interlayer distance, electrical conductivity, composition, and mechanical strength of produced MXenes.

Hence, there are numerous minor issues related to the large-scale production of MXenes, which depend upon various processing parameters. In other words, it is very challenging to transfer lab-scale technology to scalable industrial machine processing. However, few reports in the literature discuss the scalable production of MXenes and their prospects for industrial-scale fabrication.

1.2 Scalable Fabrication of MXene Through Chemical Route

The large-scale reactors for manufacturing MXenes at a massive scale are advantageous in tuning the properties, monitoring and optimizing the chemical reaction, reducing human resources, processing, safety, and low contamination. Moreover, the automated operation through a computer interface makes it easy to customize the reaction and its course and turns it into an intelligent synthesis strategy. For instance, Shuck et al. [5] reported the large-scale production of titanium carbide MXene using a custom-designed chemical reactor, as shown in Fig. 1. They prepared a large batch of MXene using an indigenous reactor and compared it with a small batch of MXene prepared through conventional lab-based chemical exfoliation.

The main parts of an indigenously designed reactor are a cooling jacket, gas inlet/outlet with screw feeder, mixer, thermocouple, and agitator. The cooling jacket is coupled with a cooling tank that allows the reaction temperature throughout the course of the reaction. The screw attached with the outlet/inlet allows the uniform addition of MAX precursor by applying downward pressure to the system. The internal reactor, including blades of mixer and thermocouple cascade, comprises Teflon to protect it from damage during HF reactions. The thermocouple allows monitoring the reaction temperature. Finally, the agitator is designed to achieve homogenous mixing of precursors during the reaction.

However, the designed reactor can be upgraded by considering advancements like replacing water with coolants in the cooling tank. In a typical synthesis, Shuck et al. [5], HF-based selective etching route is followed, resulting in $Ti_3C_2T_x$ multilayer

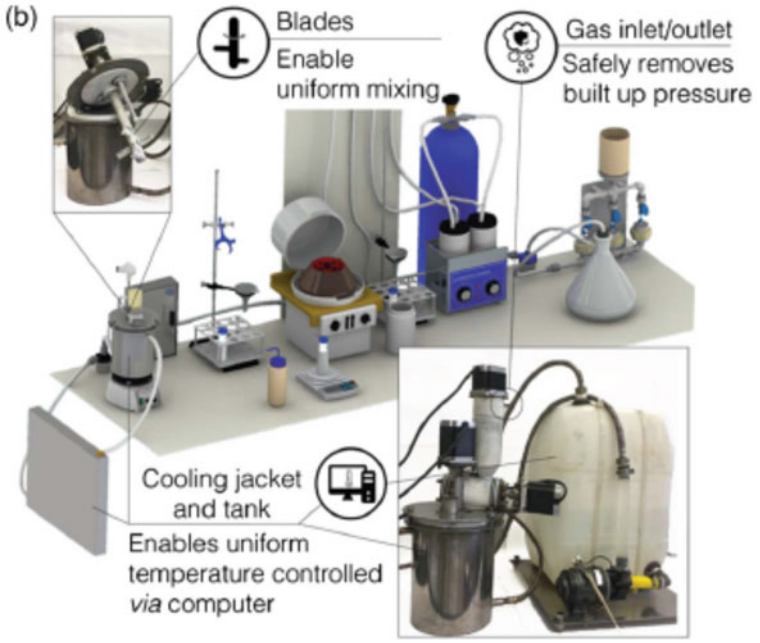

Fig. 1 Pictorial illustration of 3D model of MXene reactor for large-scale production; Reprinted with permission of [5]. Copyright 2020, Wiley

MXene and single-flake MXene for more extensive and smaller batches, respectively. Further, the synthesized MXenes were intercalated with water and vacuum dried subsequently. The yield of the larger batch was obtained be significant (52%) compared to that of the smaller batch indicating the success of the technique for mass production. XRD revealed similar structural characteristics of both the batches of MXene with all characteristic prominent peaks, as shown in Fig. 2.

Moreover, in the concerned study, XPS, UV–Visible, SEM, DLS, and Raman spectroscopies reveal that the products from both batches are identical in physicochemical characteristics [5]. Therefore, it indicates that this method can result in the mass production of MXenes without compromising their desired properties. Hence, the larger-reactor method has been proposed as a suitable technique for the scalable production of MXenes. However, the strategy has only been experimentally validated for $Ti_3C_2T_x$ -MXene and yet to be evaluated for other MXenes with similar configurations.

Furthermore, Zhang et al. [11] has reported an ammonium ion route to prevent aggregation and restacking of few-layered MXene nanosheets in large quantities. In a typical synthesis, a solution-phase flocculation method (NH^{4+} method and modified NH^{4+} method) has been adopted for large-scale production of MXenes with commercial requirements. The method is suitable for the large-scale production of various MXenes, including $Ti_3C_2T_x$, $Nb_4C_3T_x$, V_2CT_x, Nb_2CT_x, etc.

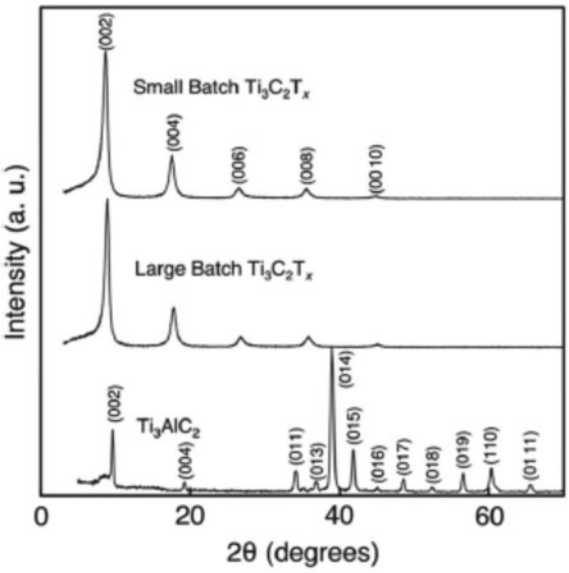

Fig. 2 Comparison of structural characteristics of the small and large batch produced $Ti_3C_2T_x$; Reproduced with permission [5]. Copyright 2020, Wiley

1.3 Scalable Synthesis of MXene Self-standing Films

There are other reports on scalable production of MXenes, their films, or hybrids with other materials aiming to meet industrial requirements both qualitatively and quantitatively [12–14]. In literature, the freestanding films of MXenes are reported to fabricate using vacuum-assisted filtration techniques [12, 15, 16]. MXene flakes are separated from their precursor solvent using a filtration membrane and vacuum pump in a typical process. However, its commercial use is limited due to several bottlenecks, including energy intensiveness, the dependence of area of film on filtration membrane, time-consuming requirements of the dedicated pump to fabricate each film, high cost, and low yield [12, 15, 16]. Other techniques used to fabricate freestanding films include natural sedimentation, spray-coating, blade-coating, and layer-by-layer assembly strategies [12, 16, 17]. However, these methods are constrained for commercial productions due to non-conductive fillers, which dramatically reduce their electrical conductivity and performance. The drop-casting technique is an attractive alternate technique to obtain MXenes films (owing to their hydrophilic nature) on the desired substrate [12, 18, 19]. However, the inverse methodology has been used to obtain self-standing MXene films on a hydrophobic surface [12]. Due to the hydrophobic nature of the substrate, the MXene interacts unfavorably with the substrate, and dried films can be easily delaminated from the substrate due to the prominent MXene-MXene interactions over MXene-substrate interactions.

Taylor et al. [12] reported the scalable fabrication of conductive freestanding $Ti_3C_2T_x$ film on a hydrophobic plastic substrate using the drop-casting technique. First, $Ti_3C_2T_x$ dispersion was prepared using the HF etching route in a typical

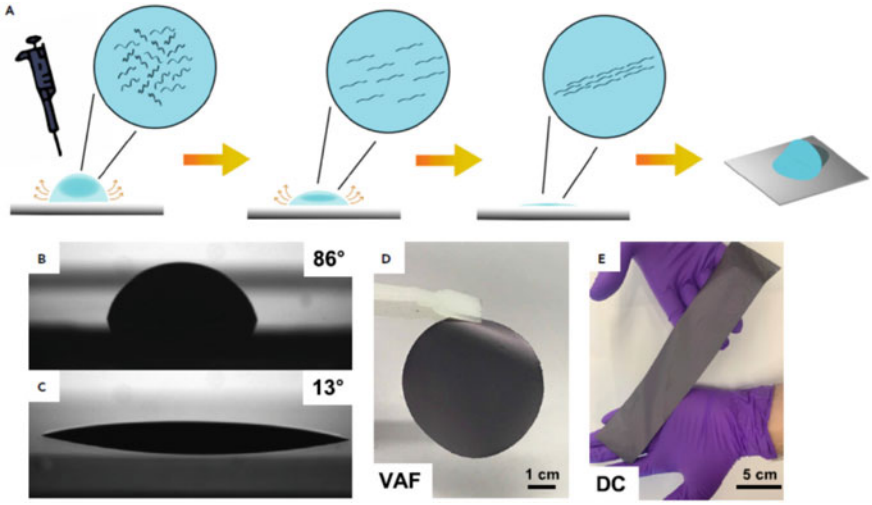

Fig. 3 Strategies to fabricate freestanding MXene films; Reproduced with permission [12]. Copyright 2020, Cell Press

synthesis. Then, the films were deposited by piping out $Ti_3C_2T_x$ dispersion over polyethylene film pulled tightly over a flat surface and subsequent drying, as shown in Fig. 3.

The physicochemical properties of obtained freestanding MXene film were significant with those prepared with the VAF route, which pints out the success of the adopted technique for scalable production. It is a cost-effective, time-saving, economical, high-yielding, and straightforward technique with commercial prospects to obtain freestanding films of MXene.

Moreover, an important fact related to MXene film scalable fabrication is prevention from the creation of voids during the synthesis. Wan et al. [14] reported a novel technique for scalable synthesis of MXene films through bridging-induced densification. The MXene layered structure was densified in a typical synthesis, and voids were removed using a sequential combination of covalent and hydrogen bonding agents. The obtained MXene films were reported to be scalable with enhanced mechanical strength and electrical conductivity with high performance in electromagnetic shielding.

1.4 Scalable Synthesis of MXene Hybrids

The scalable production of MXenes is not limited to its pristine form but has also been reported to the formation of its hybrids for diversified applications [20, 21]. For example, Levitt et al. [22] reported the synthesis of Continuous and Scalable Multifunctional MXene-Infiltrated Nanoyarns (nylon and polyurethane (PU) nanofiber

yarns) using one-step bath electrospinning technique. The fabricated MXene based nano yarns showed high-performance stain sensing with optimal stretchability and significant electrochemical properties.

For instance, Zhao et al. [23] reported the alternative stacking of MXene and reduced graphene oxide nanosheets using spray-assisted layer-by-layer assembly. The method is beneficial for fabricating significantly large, freestanding MXene/rGO heterostructured films with excellent electrochemical performance. Further, Wang et al. [24] reported the scalable synthesis of polyaniline nanodots intercalated into MXene film interlayers in the form of viscous functional inks with ultrahigh volumetric capacitance for supercapacitor applications. Similarly, various reports have reported the scalable synthesis of MXene and its nanocomposites for diversified applications, as listed in Table 1.

Hence, it is evident that the scalable synthesis strategies for MXenes are currently limited and only dedicated to $Ti_3C_2T_x$ MXene. Moreover, the scalable route to obtain pristine MXene is only achieved from the selective etching route [2, 3, 5]. However, this route results in environmental contamination due to the reactants' corrosive nature. As well, the other routes are limited in terms of yield. Hence, it is essential to design scalable routes to synthesize pristine MXene from MAX phases to meet the gap between technology and industries.

Furthermore, the fabrication of MXene films and hybrids from pre-synthesized MXene precursors has also been scaled for diversified applications. However, the studies are limited and only dedicated to specific applications. As a result, it has

Table 1 Scalable Synthesis of MXene and its hybrids

Material	Method	Application	References
$Ti_3C_2T_x$ membrane	Scalable brush-coating	Desalination and organic solvent recovery	[25]
$Ti_3C_2T_x$	Large reactor	Mass production	[5]
MXene films	Bridging induced densification	EMI shielding	[14]
$Na_{0.23}TiO_2/Ti_3C_2$ composites	In-situ transformation reaction	Lithium/sodium-ion batteries	[26]
$Ti_3C_2T_x$ MXene nanoyarns	Bath electrospinning	Strain sensor	[5]
Freestanding $Ti_3C_2T_x$ MXene films	Drop casting	EMI shielding	[12]
$Ti_3C_2T_x$ MXene inks	Extrusion printing and inkjet printing	Micro-supercapacitors	[13]
$Ti_3C_2T_x$ MXene-based on-chip	Cold laser-cutting followed by spin-coating	Energy storage	[27]
N-MXene/rGO (SNMG-40) hybrid film	Heteroatom doping strategy	Flexible energy storage device	[20]

created a large void between MXenes and their commercial use. Hence, dedicated research is essential to obtain scalable techniques for fabricating MXenes and hybrids for commercial applications.

2 Advanced Precursors for MXene Synthesis

2.1 Synthesis of MXene from Non-MAX Phases

The challenges in the scalable production of MXenes from MAX phases have led researchers to find alternative precursors for its production [2, 3, 28]. It has been reported in the literature that all the theoretically proposed MXene do not have MAX phases, especially for ternary metal carbides [2, 3, 28]. Hence, a quest to find new MAX phases and alternative precursors such as non-MAX phases has resulted in extensive research. Several transition metals such as Sc, Zr, and Hf are found in unique layered compound form $(MC)_n[Al(A)]_mC_{m-1}$ (with 'n' as same meaning discussed for MAX phases, 'm' id 3,4, and A is Si/Ge) instead of MAX phases [28]. Various Non-max precursors to synthesize MXenes have been listed in Table 2.

These Non-MAX phases are layered uniquely with Al (A)-C sublayers [28]. The non-MAX phase of $M_{n+1}AlC_n$ possesses Al layers intercalated by strong M-bonding layers, as shown in Fig. 4. However, other forms of non-MAX phase, i.e. $(MC)_n[Al(A)]_mC_{m-1}$ possess carbon shared with transition materials with AL (A) at their boundaries. It has been reported that the non-MAX phase $Zr_3Al_3C_5$ can be prepared by PES of Zr, Al, and graphite powders for the synthesis of the $Zr_3C_2T_x$ [28].

Table 2 List of reported Non-MAX phases based MXenes in literature

S. no.	Non-MAX precursors			Derived MXene
1	Zirconium-based [2, 28–30]	Al contained	$Zr_2Al_3C_4$ $Zr_3Al_3C_5$ $ZrAl_8C_7$ $ZrAl_4C_4$ $Zr_2Al_4C_5$ $Zr_3Al_4C_6$	Zr_2C_4 Zr_3C_5 ZrC_7 ZrC_4 Zr_2C_5, Zr_3C_6
		Al (A) contained	$Zr_2[Al\ (Si)]_4C_5$ $Zr_3[Al\ (Si)]_4C_6$ $[ZrY)]_2Al_4C_5$ $Zr_2[Al\ (Ge)]_4C_5$ $Zr_3[Al\ (Ge)]_4C_6$ $Zr[Al\ (Si)]_8C_7$	Zr_2C_5 Zr_3C_6 $[ZrY)]_2C_5$ Zr_2C_5 Zr_3C_6 ZrC_7
2	Hafnium-based [28]	Al contained	$Hf_2Al_4C_5$ $Hf_3Al_4C_6$ $HfAl_4$ $Hf_2Al_3C_4$	Hf_2C_5 Hf_3C_6 HfC_4 Hf_2C_4

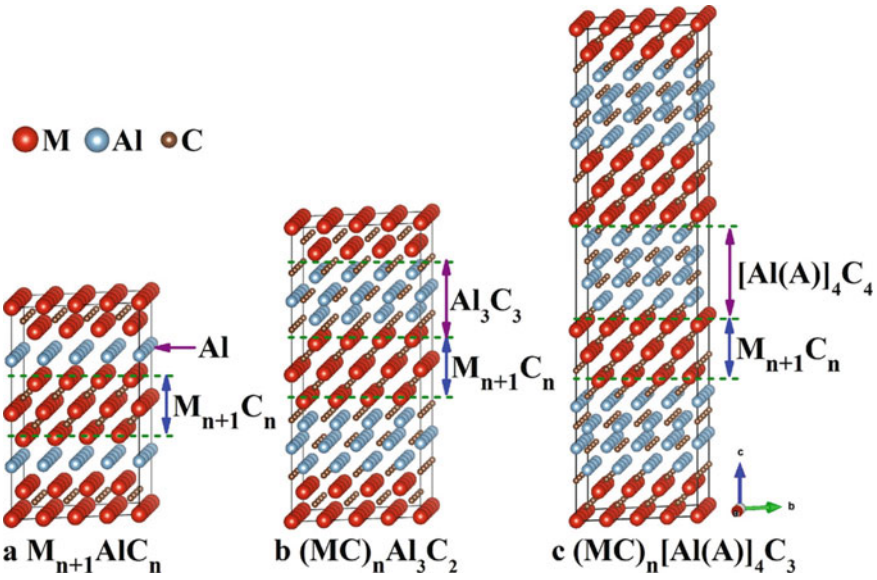

Fig. 4 Selective etching of a M_3AX_2 layered precursor to yield M_3X_2 MXene; Reproduced with permission [28]. Copyright 2019, Springer

Furthermore, the etching of '*A-C*' from the non-MAX phase is more conducive and convenient than the etching of 'A' element from MAX phases. It has also been shown the etching of 'A-C' to fabricate U_2CT_x MXene from $U_2Al_3C_4$ non-MAX phase is cost-effective and straightforward [28]. This etching strategy can be done through chemical reactions amongst HCl and molten LiF salt, which successfully remove the 'A' group more safely with very few defects. It results in large flake MXenes and develops large spacing amongst its layers due to intercalation with cations like Li^+. It has also been reported to modify and enhance its surface functionalities.

2.2 Fabrication from "i-MAX" Phases

Recently a new MAX phase termed "i-MAX" has been reported as a precursor for synthesizing MXenes [3, 31–34]. These are in-plane chemically ordered forms of MAX phases described by a general formula of "$(M^1_{2/3}M^2_{1/3})_2AX$" with M's as two different chemically ordered in-plane transition metals [32]. Since M^2 elements are present amongst the traditional 'A' elements and 'M' elements in the periodic table. They can be etched together with the 'A' layer by regulating the etching conditions during the formation of MXenes from 'i-MXenes'. It offers a way to comprehend 2-D materials with in-plane chemical order/ordered vacancies. Rosen et al. [32] reported the selective etching of Al and Sc atoms from in-plane chemically ordered "i-MXene" phase, i.e. $(Mo_{2/3}Sc_{1/3})_2AlC$ through 48 wt.% LiF/HCl or HF.

However, the etching time is different for the etchants (24 at room temperature and 48 h at 35 °C). It has resulted in the formation of 2-D $Mo_{1.33}CT_x$ nanosheets with ordered in-plane metal vacancies. However, the etching of MXene from 'i-MAX' is limited. For instance, $(V_{2/3}Sc_{1/3})_2AlC$ is soluble in numerous etchants such as 48 et% HF, HCl/NaF, and HCl/LiF at room temperature a MAX phase with less Sc content can be etched into $V_{2-x}C$ under the same circumstances [32]. Other "i-MAX" phases reported in the literature include $(Cr_{2/3}Sc_{1/3})_2AlC$, $(Cr_{2/3}Y_{1/3})_2AlC$, $(Mo_{2/3}Sc_{1/3})_2GaC$, $(Mo_{2/3}Y_{1/3})_2GaC$, and $(Cr_{2/3}Zr_{1/3})_2AlC$ [3, 32–34]. The structural design of MXenes can be realized at an atomic scale by exploring the etching of 'i-MAX' phases and bringing new prospects to develop scalable methods to develop MXenes.

3 MXenes in Wearable Electronics

Wearable electronics owing to excellent mechanical compliance and exceptional sensitivity, have attracted immense attention of the scientific community to design the next-generation devices for healthcare, automobiles, robotics, and prosthetics [35–38]. It requires flexible surface-mounted wearable devices with a compact design with consistent electrical characteristics under cyclic strain situations during regular movements [39, 40]. It has constrained the traditional use of silicon in manufacturing such surfaces and generated a quest to search for advanced nanomaterials with reliable physicochemical characteristics. MXenes have recently emerged as the material of interest to architect wearable devices like physical sensors, chemical sensors, and biosensors due to their unique physicochemical properties [38, 41–43]. MXenes have been reported to indulge in diversified applications, including health, environmental, and motion monitoring [38, 41, 43, 44]. The diversified range of applications of MXenes in wearable devices is due to their unique properties like layered 2-D morphology, tunable electrical and thermal conductivity, abundance of surface chemistries, variable interlayer distance, mechanical stability, and hydrophilicity [43, 45].

Furthermore, rich surface functionalities of MXenes allow appropriate surface modifications/functionalization and performs multi-interactions with target molecules [46]. It allows the tuning of MXene physicochemical nature as per desired targeted application with enhanced performance. Moreover, the high effective surface area and numerous functional groups on MXene surface catalysis their surface interaction with target signals resulting in superior surface phenomenon-based sensing performances [43, 47, 48]. Hence, MXenes have been extensively used in wearable electronics, especially in diversified sensors, including physical, chemical and biosensors.

3.1 Flexible Physical Sensors

MXenes synthesized using chemical etching usually exhibit several physicochemical properties superior or comparable to graphene, including hydrophilic nature, electronic properties, bendable strength, oxidation resistance, and electron irradiation resistance [39, 47]. As a result of its superior electrical properties, MXene is utilised in strain sensors to detect minor form variations. MXenes can also be machine processed swiftly due to their hydrophilic character. They can also be combined with other materials like polymers to attain the desired flexibility [41, 49]. Hence, MXenes have attracted the excessive interest of the scientific community towards physical sensors.

3.1.1 Flexible Strain Sensor

A flexible strain sensor works on the principle of transforming the tensile strength of the device into the resistance signal as output [50]. The applied external force cracks the sensor's internal conductive channel, resulting in a change in electrical properties [51]. MXenes are layered structures stacked together due to interaction forces like Vander Waal forces in a 2-D fashion [3]. The application of external stress on MXenes in the vicinity of effective sliding results in the formation of large cracks. It results in the breaking of conducting channels amongst MXene layers generating an output signal in the form of resistance variation. Generally, the sensitivity of the strain sensor is measured in terms of its gauge factor (G) given by [47]

$$G = \frac{\frac{\Delta r}{r_o}}{\frac{\Delta l}{l_o}}$$

with Δr/or representing variation in resistivity, where 'Δr' is the difference in resistivity after and before application of strain, 'or is the resistivity of the sensor at rest without applying strain, and 'Δl' is the absolute variation in length with 'l_o' as the original length without application of strain.

However, the common problem with designing wearable MXene based devices is the stacking of its layer and less flexibility [41]. It is often addressed by introducing a second phase material of different dimensions into the MXene layers. Various nanomaterials have been reported for use as intercalants to prevent stacking of MXene layers and provide flexibility. These nanomaterials include macromolecules, carbon nanostructures like carbon nanotubes (CNT), graphene and its derivatives, metal ions, and metal-based nanostructures [43, 46, 52, 53]. However, flexibility has been attained by using polymer substrates or fabricating their hybrid nanocomposites. For instance, Cai et al. [54] reported prevention of stacking of $Ti_3C_2T_x$ MXene layers by intercalating with hydrophilic single-walled carbon nanotubes (SWCNT) using a layer-by-layer spray coating strategy. The obtained structure is with disorderly

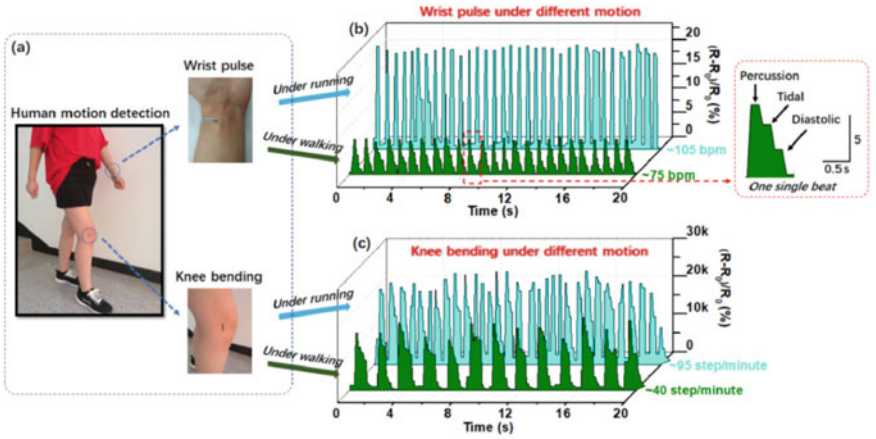

Fig. 5 Silver nanowire/$Ti_3C_2T_x$/Ni^{2+} based nacre-mimetic strain sensor; Reproduced with permission [44]. Copyright 2019, American Chemical Society

distributed SWCNT amongst the layers forming a conductive network. It has been evaluated as a strain sensor with sensitivity up to 64.6 in the range 0–30% of applied strain and 772.60 in 40–70% applied strain.

On the other hand, An et al. [55] achieved flexibility for $Ti_3C_2T_x$ nanosheets-based strain sensor through including poly (diallyl dimethylammonium chloride) (PDAC) using the LBL strategy. Further, the fabricated nanocomposites were loaded on different substrates, including polydimethylsiloxane (PDMS), indium tin oxide (ITO), silicon and polyethylene terephthalate (PET). As a result, the $Ti_3C_2T_x$/PDAC/PDMS-based strain sensor showed superior stretching performance up to 40%, whereas $Ti_3C_2T_x$/PDAC/PET sensor showed superior bending performance up to 35%. Furthermore, Shi et al. [44] fabricated silver nanowire/$Ti_3C_2T_x$ and introduced dopamine and nickel ions (Ni^{2+}) to architect a nacre-mimetic strain sensor, as shown in Fig. 5.

The reported sensitivity range is more than 200 for a whole applied strain range, which is superior to most of the reported flexible sensors in the literature. Hence, the addition of different dimensional amongst MXene sheets forms conducting network and prevents restacking, whereas polymer inclusion provides flexibility. Therefore, it endows the strain sensing performance of MXenes with optimal flexibility for wearable electronics.

Alternatively, Zhang et al. [56] reported using $Ti_3C_2T_x$ and polyvinylalcohol (PVA) hydrogel to achieve excellent stretchability, superior flexibility, and self-repair ability in fabricated strain sensors. The tensile strength of $Ti_3C_2T_x$/PVA hydrogel was 3400%, owing to cross-linking between surface end functionalities of $Ti_3C_2T_x$ and PVA hydrogel. Furthermore, the GF of the strain sensor in the range of 0–0.5 and 0.5–3.0% were reported to be 60–80 and 21, respectively. Similarly, Liao et al. reported evaluation of $Ti_3C_2T_x$/polyacrylamide/PVA hydrogel-based strain sensor with an excellent sensitivity of 44.85 with self-healing capabilities. Hence, the MXenes

possess the colossal potential to develop next-generation flexible strain sensors and enhance their sensing performances by fabricating nanocomposites and hydrogels.

3.1.2 Flexible Pressure Sensor

Flexible pressure sensors are generally piezoresistive in nature [57]. The application of external pressure on the sensor produces deformation in the material resulting in an output resistance signal [42, 56]. The sensitivity of pressure sensors is calculated similarly to the aforementioned for strain sensors [47]. Majorly the flexibility for pressure sensors is achieved by either using flexible polymer substrates such as PE, PET, PDMS or using aerogels [39]. For instance, Ma et al. [58] reported a flexible pressure sensor synthesized from multilayer $Ti_3C_2T_x$ on the polyimide (PI) integrated electrode substrate with the sensitivity of 180.1–94.8 and 94.8–45.9 in the range of 0.19–0.82 and 0.82–2.13%, respectively.

Furthermore, Yue et al. [59] reported piezoresistive pressure sensor based on MXene-sponge-PVA nanowires with ultrahigh sensitivity of 147 and 142 in the pressure range of 0–5.37 and 5.37–18.56 kPa, respectively. Guo et al. [60] fabricated a degradable transient pressure sensor based on polylactic acid (PLA)/MXene sandwiched structure. Alternatively, MXene based aerogels possessing high porosity and superelasticity are emerging for fabricating flexible pressure sensors. For instance, Ma et al. [61] reported $Ti_3C_2T_x$/rGO aerogel-based flexible pressure sensor with excellent sensing performance, as shown in Fig. 6. It is attributed to the synergistic effects of rGO providing high mechanical strength for the aerosol skeleton and $Ti_3C_2T_x$ providing high conductivity for a strong resistance output signal.

Furthermore, there are reports on the in-situ growth of MXenes in aerogels to fabricate pressure sensors. Wang et al. [62] reported skin-inspired $Ti_3C_2T_x$/natural microcapsule composite film with superior mechanical deformability, which mimics the structure and functionality of human skin. Hence, the main strategies to architect flexible pressure sensors using MXenes and their derivatives include aerogels and elastic substrates.

3.2 Wearable Biosensors

Wearable biosensors possess enormous potential in developing point-of-care advanced diagnostics and sensing strategies for rapid and economical detection [38]. Lately, MXenes have emerged as a potential candidate for developing wearable biosensors for various applications. For instance, Chen et al. [63] reported an intracellular pH detecting sensor based on $Ti_3C_2T_x$ quantum dots using a ratiometric photoluminescence probe. Lei et al. [64] reported an ultrasensitive enzymatic wearable sensor based on MXene/Prussian blue hybrid for glucose and lactate detection. They implemented a solid–liquid-air three-phase strategy to achieve a sufficient oxygen

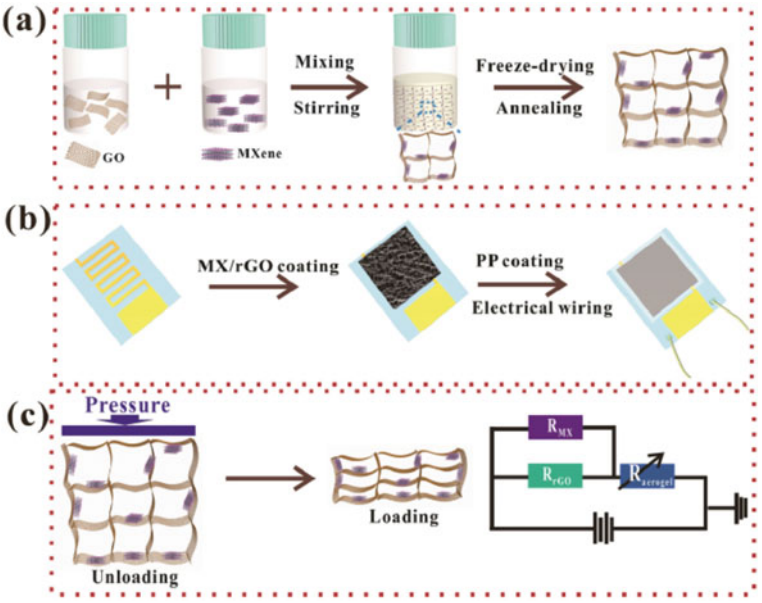

Fig. 6 Fabrication of $Ti_3C_2T_x$/rGO aerogel-based flexible pressure sensor; Reproduced with permission [61]. Copyright 2018, American Chemical Society

supply, increasing the biosensor's sensitivity. The achieved sensitivity using electrochemical techniques of 35.3 $\mu A\ mm^{-1}\ cm^{-2}$ for glucose and 11.4 $\mu A\ mm^{-1}\ cm^{-2}$ for lactate signify the strong prospect in personalized healthcare monitoring using wearable technology biosensors. Recently, Yang et al. [65] reported a hospital-on-chip system with multifunctional microneedle electrodes based on MXene nanosheets, as shown in Fig. 7. The reported biosensor was integrated on a single chip for enhanced diagnostics and therapies resembling a miniature hospital. The microneedles in this miniature system are used as a transdermal and painless patch to puncture dead skin, which acts as a barrier during drug delivery. In addition, it has been reported to sense the slight potential difference created in the body due to human arm muscle contraction and human eyes movement. Hence, the biosensor served two primary purposes required for medical treatment, including drug delivery and biosensing.

Furthermore, Zhang et al. [50] reported a hydrogel-based biosensor fabricated from polyvinyl alcohol, cellulose nanofibril, MXene nanosheets, and glycerol with significant electrical conductivity (2.58 mS cm^{-1}) and flexibility even at −18 °C. The biosensor exhibited high sensitivity (2.30), rapid response (0.165 s), inclusive working strain range (559%), good linearity (0.999), lower strain detecting range (1–5%), and varied operating temperature range (−18 to 60 °C). On the other hand, Soomro et al. [66] reported a biosensor based on TiO_2/MXene-$BiVO_4$ hybrid for robust detection of soluble CD44 proteins using photoelectrochemical strategy. The interfacial assembly was the epitome for stimulating fast charge carrier transfer from

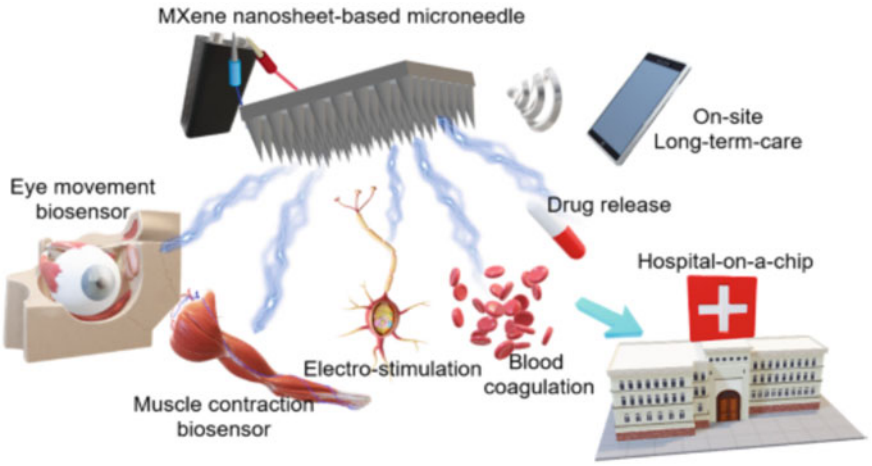

Fig. 7 Concept of hospital-on-chip using MXene nanosheets; Reproduced with permission [65]. Copyright 2021, American Chemical Society

photo-excited $BiVO_4$ and TiO_2 to $Ti_3C_2T_x$ Sheets, resulting in an energy level-cascade that allows negligible charge-carrier recombination besides strong photocatalytic redox reactions. The sensor detected a vast concentration CD44 window of $2.2 \times 10 - 4$ ng mL^{-1} to 3.2 ng mL^{-1} with a low detection limit of $1.4 \times 10 - 2$ pg mL^{-1} signifying its reliable clinical applicability. Hence, MXene and its hybrids possess tremendous potential in developing wearable biosensors for personalized healthcare monitoring and compact diagnostic techniques. However, the research is in its infancy, and it is required to be incorporated with advanced intelligent features and required dedicated clinical trials.

3.3 Wearable Chemical Sensors

MXene and its hybrids have been extensively reported for designing flexible gas/vapor/chemical species detecting sensors for diversified applications such as healthcare, environmental, safety, and agricultural monitoring [42, 43, 47]. This tremendous potential of MXene based materials for flexible chemical sensors has already been massively reviewed in numerous literature reports [43, 46, 47, 67]. However, their applicability for wearable devices is yet to be done for practical applications and at its infancy. The attainment of flexibility and stretchability is similar to that of physical and biosensors by using secondary materials like macromolecules or flexible substrates [52, 68]. Furthermore, the application of MXenes is not limited to gas/vapor sensing but also extended to water remediation application by removing heavy metal ions and radionuclides [69, 70]. Since the reports are extensive, they have been summarized in Table 3 for a broad outlook. Table 3 represents the compre-

Table 3 Flexible sensors based on MXene and its hybrids to detect gases and VOCs

Sensing material	VOC	Sensitivity (%)	Concentration	Recovery/response time
3TTP [71]	Methanol	2.7%	5 ppm	~1.5/1.7 min
	Ammonia	0.7	10 ppm	NR
	Nitrogen Dioxide	0.9	10 ppm	NR
	Acetone	0.08%	5 ppm	~1.5/1.7 min
$Ti_3C_2T_x$- PANI Sensor [72]	Ethanol	1.56%	1 ppm	0.4 s/0.5 s
	Ammonia	20	200 ppm	NR
PANI/$Ti_3C_2T_x$ [73]	Formaldehyde	0.2%	25 ppm	NR
	Hydrogen Sulfide	1	25 ppm	NR
PEDOT:PSS/$Ti_3C_2T_x$ [74]	Ammonia	0.05	25 ppb	~600 s/1400 s for 25 ppb
	Sulfur Dioxide	~0.02	25 ppm	NR
	Carbon Monoxide	~0.05	25 ppm	NR
	Carbon Dioxide	~0.01	10%	NR
Cationic polyacrylamide/$Ti_3C_2T_x$ [75]	Methanol	15%	2000 ppm	NR
	Ethanol	10%	2000 ppm	NR
	Acetone	10%	2000 ppm	NR
	Ammonia	1.5	50 ppm	~12–14 s for 150 ppm
Ti3C2Tx/ZnO spheres [76]	NO_2	41.93%	100 ppm	~34 s
Ti3C2Tx MXene/graphene hybrid fibers [20]	Ammonia	~600%	50 ppm	~20 min
Ti3C2Tx MXene@Pd [77]	Hydrogen	$(23.0 \pm 4.0)\%$	4% H_2	(32 ± 7) s
MXene/rGO/CuO hybrid aerogels [53]	Acetone	52.09%	100 ppm	~7.5 s

hensive outlook of flexible gas/vapor sensors reported experimentally for gas/volatile organic compound sensing using MXene based materials.

Although most of the reports mentioned in Table 3 have been anticipated for designing high-performance wearable gas/vapor sensors, the wearability of the device has not been explored. However, few reports address the MXene based sensors with wearable features. For instance, Tang et al. [6] reported wearable and stretchable VOC sensors based on MXene/polyurethane (PU) core-sheath fibers for efficient detection of acetone using the conductometric mode, as shown in Fig. 8.

The sensor exhibited excellent sensitivity (5–325 fold higher than planer MXene based sensor) towards a wide range of acetone (ppb level to saturated vapor) with

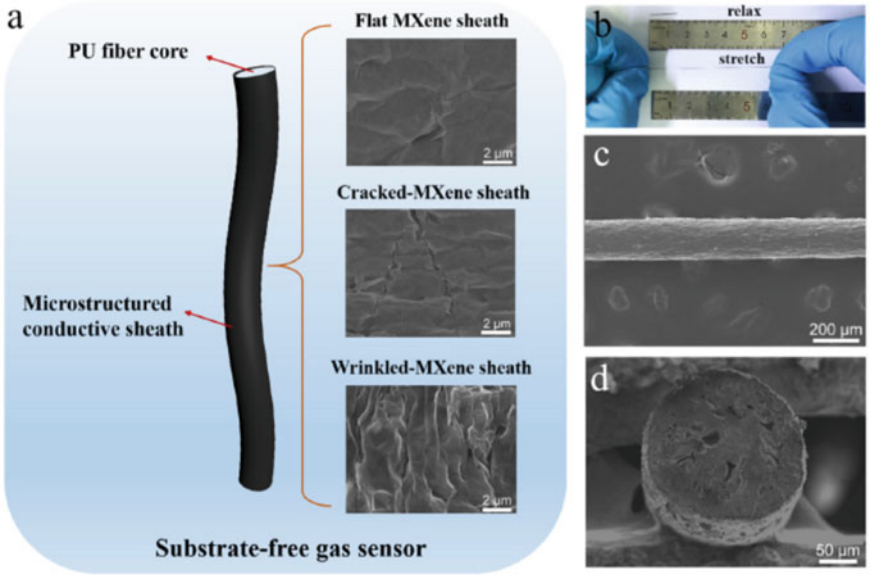

Fig. 8 MXene/polyurethane (PU) core-sheath fibers based conductometric sensor for detecting acetone; Reproduced with permission [6]. Copyright 2021, Elsevier

a high signal-to-noise ratio (SNR, 160% higher than planer MXene based sensor). Moreover, they introduced microcracks on the conductive fiber sheath, which can take deformation in human skin (30%) with a negligible sensing interference from generated tensile strain. Zhang et al. [78] reported ZnO/MXene nanowire (NW) arrays piezoelectric nanogenerator (PENG) driven formaldehyde sensor based on MXene/Co_3O_4 composite. The sensor exhibited excellent sensitivity of 52% towards 0.01 ppm of formaldehyde with rapid recovery (~5 s). The potential of the sensor for the self-driven and wearable feature was elaborately presented.

Furthermore, Zhang et al. [79] reported a latex/polytetrafluoroethylene-based triboelectric nanogenerators driven $Ti_3C_2T_x$ MXene/metal–organic framework-derived copper oxide (CuO) ammonia sensor. The self-driven NH3 sensor through TENG has an excellent response (V_g/V_a = 24.8 @ 100 ppm) at room temperature and shows an excessive potential in observing pork quality. On the other hand, Li et al. [80] reported a termination-modified $Ti_3C_2T_x$ VOC sensor for wearable ethanol monitoring in human exhaled breath. These reports demonstrate the potential of MXenes based sensing materials for architecting next-generation wearable medical electronics and intelligent healthcare. However, mass production and assessing performance with clinical data require extensive dedication for their practical applications.

4 MXenes in Wireless Communication

The developments of wearable devices are not limited to achieving flexibility and stretchability. It is essential to include internet-of-things (IoT) to design intelligent wearable devices, which use radio-frequency (RF) antennas [47, 81, 82]. Traditionally, metals like copper, silver, aluminum are used to design RF antennas owing to their excellent electrical conductivity. However, the intrinsic skin effect due to the thickness of these materials limits their commercial applicability. Due to the frequency dependence of skin depth, the thickness of metal-based antennas must be at least ~5 μm for these applications ensuring adequate space for the flow of charge carriers [81]. Recently, highly conducting 2-D nanomaterials such as MXenes possess the potential to develop next-generation compact, lightweight, portable, and flexible RF antennas [81–84]. It is attributed to their solution processability, excellent electrical conductivity, and rich surface functionalities. MXenes based negatively charged flakes possess ξ potential from −30 to −80 mV, which can be processed using various techniques such as spray coating, spin coating, drop-casting, and printing for RF applications [81, 83–85].

Sarychev et al. [81] reported the first dipole antenna based on MXenes of thickness in the range 62 nm–8 μm, operating in the Bluetooth and WiFi frequency bands at 2.4 GHz. They also fabricated a 1-μm-thick MXene RF identification device tag reaching a reading distance of 8 m at 860 MHz. They described a one-step spray approach for producing MXene-based antennas using MXene water-based colloidal ink. The fabricated antenna performed even at a considerably lower thickness (62 nm), reaching a gain of −7 dB, indicating that the MXene based antennas work at a shallow thickness than that of other reported materials possessing tremendous potential to develop next-generation ultrathin and transparent wireless devices. Li et al. [84] reported a stretchable SWCNT/MXene based dipole antenna with the uniaxial stretchability of 150% with unaffected reflected power <0.1%. Furthermore, they integrated this antenna with SWCNT/MXene electromagnetic shields (with shielding performance of 30–52 dB) to fabricate a mechanically stable wireless transmission system while attenuating the human body's EM absorption shown in Fig. 9.

On the other hand, Han et al. [83] reported $Ti_3C_2T_x$ MXene based microstrip transmission lines with less energy attenuation and patch antennas with high-power radiation in the frequency range of 5.6–16.4 GHz. The radiation efficiency of fabricated 5.5 μm thick MXene based patch antenna was comparable with standard 35 μm thick copper patch antenna at 16.4 GHz. They further demonstrated significant performance of MXene patch antenna array with integrated feeding circuits on a conformal surface at 28 GHz, which is required in practical 5G applications. Fu et al. [82] fabricated conductive fibers with MXene sheaths and alginate cores for developing wearable heaters and wireless communication systems using a cation-induced assembly strategy. Hence, MXenes, due to their excellent conductivity, tunable surface functionalities, and hydrophilic nature, possess the potential

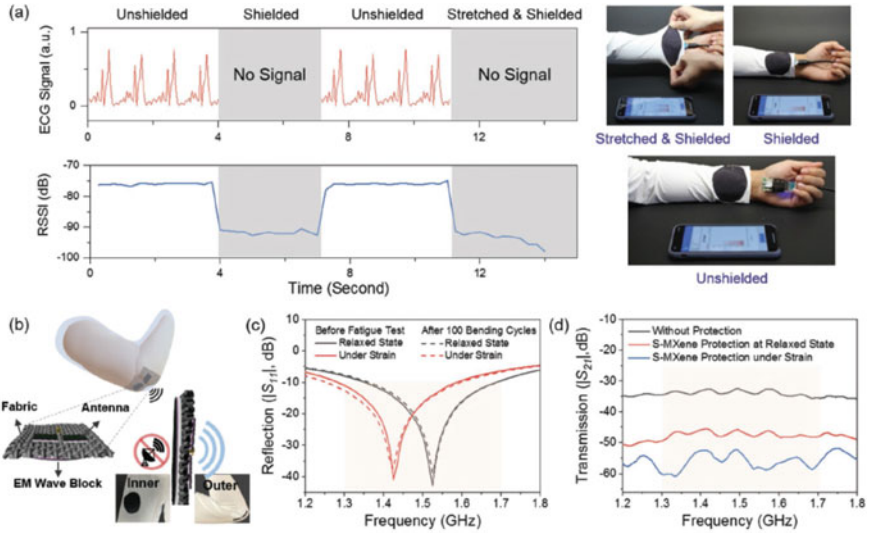

Fig. 9 Wearable Electronics using MXene based materials; Reproduced with permission [84]. Copyright 2020, Wiley

to be processed for architecting next-generation intelligent wireless communication systems.

5 Conclusions and Prospects

MXenes owing to their unique and tunable physicochemical characteristics like electrical conductivity, thermal stability, rich surface functionalities, good mechanical strength, and high effective surface area, have been used for developing next-generation wearable devices. Furthermore, their hydrophilic nature helps in machine processability and device fabrication. However, the first requirement is the scalable synthesis of MXene based materials, which is achieved using chemical etching strategies. These methods are limited by costing secondary contamination to the environment through byproducts, which raises safety concerns for manufacturers and users. It has raised a quest to explore alternative precursors like non-MAX and 'i-MAX' phases and advanced fabrication strategies like green synthesis and one-pot large reactor synthesis. Further, the requirement of flexibility and stretchability is achieved by either fabricating MXene-macromolecule hybrids or using flexible substrates. The optimum flexibility of these MXene-based materials is used to manufacture wearable electronic devices like physical, chemical, and biosensors. Owing to large effective surface area and rich surface chemistries, these materials exhibit excellent surface activities resulting in excellent sensing performances for strain, pressure, gas, volatile organic vapor, humidity, and biomolecule monitoring.

The advancement of these sensors is further done by including internet-of-things and designing wireless communication systems leading to developing intelligent wearable devices. Hence, MXene based materials with optimum flexibility open new prospects for commercially architecting next-generation intelligent field-deployable wearable devices with consistent performance in every harsh condition.

References

1. Chaudhary, V., Kaushik, A., Furukawa, H., Khosla, A.: Review—Towards 5th Generation AI and IoT Driven Sustainable Intelligent Sensors Based on 2D MXenes and Borophene. ECS Sens. Plus **1** (2022)
2. Naguib, M., Barsoum, M.W., Gogotsi, Y.: Ten years of progress in the synthesis and development of MXenes. Adv. Mater. **33**(39) (2021)
3. Wei, Y., Zhang, P., Soomro, R.A., Zhu, Q., Xu, B.: Advances in the synthesis of 2D MXenes. Adv. Mater. **33** (2021)
4. Seth, Y., Dharaskar, X., Chaudhary, V., Khalid, M., Walvekar, R.: Prospects of titanium carbide-based MXene in heavy metal ion and radionuclide adsorption for wastewater remediation: A review. Chemosphere **293** (2022)
5. Shuck, C.E., Sarycheva, A., Anayee, M., Levitt, A., Zhu, Y., Uzun, S., et al.: Scalable synthesis of $Ti_3C_2T_x$ MXene. Adv. Eng. Mater. **22**(3) (2020)
6. Tang, Y., Xu, Y., Yang, J., Song, Y., Yin, F., Yuan, W.: Stretchable and wearable conductometric VOC sensors based on microstructured MXene/polyurethane core-sheath fibers. Sens. Actuators B Chem. **1**, 346 (2021)
7. Hope, M.A., Forse, A.C., Griffith, K.J., Lukatskaya, M.R., Ghidiu, M., Gogotsi, Y., et al.: NMR reveals the surface functionalisation of Ti_3C_2 MXene. Phys. Chem. Chem. Phys. **18**(7) (2016)
8. Rao, K.S.M.S.R., Joshi, J.B.: Liquid phase mixing in mechanically agitated vessels. Chem. Eng. Commun. **74**(1) (1988)
9. Jaszczur, M., Młynarczykowska, A.: A general review of the current development of mechanically agitated vessels. Processes **8** (2020)
10. Gygax, R.: Chemical reaction engineering for safety. Chem. Eng. Sci. **43**(8) (1988)
11. Zhang, S., Huang, P., Wang, J., Zhuang, Z., Zhang, Z., Han, W.Q.: Fast and universal solution-phase flocculation strategy for scalable synthesis of various few-layered MXene powders. J. Phys. Chem. Lett. **11**(4) (2020)
12. Lipton, J., Röhr, J.A., Dang, V., Goad, A., Maleski, K., Lavini, F., et al.: Scalable, highly conductive, and micropatternable MXene films for enhanced electromagnetic interference shielding. Matter **3**(2) (2020)
13. Zhang, C. (John), McKeon, L., Kremer, M.P., Park, S.H., Ronan, O., Seral-Ascaso, A., et al.: Additive-free MXene inks and direct printing of micro-supercapacitors. Nat. Commun. **10**(1) (2019)
14. Wan, S., Li, X., Chen, Y., Liu, N., Du, Y., Dou, S., et al.: High-strength scalable MXene films through bridging-induced densification. Science **374**(6563) (2021)
15. Ding, L., Wei, Y., Wang, Y., Chen, H., Caro, J., Wang, H.: A two-dimensional lamellar membrane: MXene nanosheet stacks. Angew. Chemie Int. Ed. **56**(7) (2017)
16. Ling, Z., Ren, C.E., Zhao, M.Q., Yang, J., Giammarco, J.M., Qiu, J., et al.: Flexible and conductive MXene films and nanocomposites with high capacitance. Proc. Natl. Acad. Sci. USA **111**(47) (2014)
17. Li, C., Kota, S., Hu, C., Barsoum, M.W.: On the synthesis of low-cost, titanium-based mxenes. J. Ceram Sci. Technol. **7**(3) (2016)
18. Akuzum, B., Maleski, K., Anasori, B., Lelyukh, P., Alvarez, N.J., Kumbur, E.C., et al.: Rheological characteristics of 2D titanium carbide (MXene) dispersions: a guide for processing MXenes. ACS Nano. **12**(3) (2018)

19. Yu, M., Feng, X.: Scalable manufacturing of MXene films: moving toward industrialization. Matter **3**(2) (2020)
20. Liao, L., Jiang, D., Zheng, K., Zhang, M., Liu, J.: Industry-scale and environmentally stable $Ti_3C_2T_x$ MXene based film for flexible energy storage devices. Adv. Funct. Mater. **31**(35) (2021)
21. Lee, S.H., Eom, W., Shin, H., Ambade, R.B., Bang, J.H., Kim, H.W., et al.: Room-temperature, highly durable $Ti_3C_2T_x$ MXene/graphene hybrid fibers for NH3 gas sensing. ACS Appl Mater Interfaces **12**(9), 10434–10442 (2020)
22. Levitt, A., Seyedin, S., Zhang, J., Wang, X., Razal, J.M., Dion, G., et al.: Bath electrospinning of continuous and scalable multifunctional MXene-infiltrated nanoyarns. Small **16**(26) (2020)
23. Zhao, M.Q., Trainor, N., Ren, C.E., Torelli, M., Anasori, B., Gogotsi, Y.: Scalable manufacturing of large and flexible sheets of MXene/graphene heterostructures. Adv. Mater. Technol. **4**(5) (2019)
24. Wang, Y., Wang, X., Li, X., Bai, Y., Xiao, H., Liu, Y., et al.: Scalable fabrication of polyaniline nanodots decorated MXene film electrodes enabled by viscous functional inks for high-energy-density asymmetric supercapacitors. Chem. Eng. J. **405** (2021)
25. Wu, X., Ding, M., Xu, H., Yang, W., Zhang, K., Tian, H., et al.: Scalable $Ti_3C_2T_x$ MXene interlayered forward osmosis membranes for enhanced water purification and organic solvent recovery. ACS Nano. **14**(7) (2020)
26. Huang, J., Meng, R., Zu, L., Wang, Z., Feng, N., Yang, Z., et al.: Sandwich-like $Na_{0.23}TiO_2$ nanobelt/Ti_3C_2 MXene composites from a scalable in situ transformation reaction for long-life high-rate lithium/sodium-ion batteries. Nano Energy. **46** (2018)
27. Huang, H., He, J., Wang, Z., Zhang, H., Jin, L., Chen, N., et al.: Scalable, and low-cost treating-cutting-coating manufacture platform for MXene-based on-chip micro-supercapacitors. Nano Energy. **69** (2020).
28. Zha, X.H., Zhou, J., Eklund, P., Bai, X., Du, S., Huang, Q.: Non-MAX phase precursors for MXenes. In: 2D Metal Carbides and Nitrides (MXenes): Structure, Properties and Applications (2019)
29. Gao, G., , G., Li, J., Yao, K., Wu, M., Qian, M.: Monolayer MXenes: promising half-metals and spin gapless semiconductors. Nanoscale **8**(16) (2016)
30. Zhou, J., Zha, X., Chen, F.Y., Ye, Q., Eklund, P., Du, S., et al.: A two-dimensional zirconium carbide by selective etching of Al_3C_3 from nanolaminated $Zr_3Al_3C_5$. Angew. Chemie Int. Ed. **55**(16) (2016)
31. Sokol, M., Natu, V., Kota, S., Barsoum, M.W.: On the chemical diversity of the MAX phases. Trends Chem **1** (2019)
32. Ahmed, B., El Ghazaly, A., Rosen, J.: i-MXenes for energy storage and catalysis. Adv. Funct. Mater. **30** (2020)
33. Thörnberg, J., Halim, J., Lu, J., , R., Palisaitis, J., Hultman, L., et al.: Synthesis of $(V_{2/3}Sc_{1/3})_2AlC$ i-MAX phase and $V_{2-x}C$ MXene scrolls. Nanoscale **11**(31) (2019)
34. Meshkian, R., Dahlqvist, M., Lu, J., Wickman, B., Halim, J., Thörnberg, J., et al.: W-based atomic laminates and their 2D derivative $W_{1.33}C$ MXene with vacancy ordering. Adv. Mater. **30**(21) (2018)
35. Tan, P., Zou, Y., Fan, Y., Li, Z.: Self-powered wearable electronics. Wearable Technol. **1** (2020)
36. Gu, Y., Zhang, T., Chen, H., Wang, F., Pu, Y., Gao, C., et al.: Mini review on flexible and wearable electronics for monitoring human health information. Nanoscale Res. Lett. **14** (2019)
37. Neupane, G.P., Yildirim, T., Zhang, L., Lu, Y.: Emerging 2D MXene/organic heterostructures for future nanodevices. Adv. Funct. Mater. **30** (2020)
38. Khunger, A., Kaur, N., Mishra, Y.K., Ram Chaudhary, G., Kaushik, A.: Perspective and prospects of 2D MXenes for smart biosensing. Mater. Lett. **304** (2021)
39. Xin, M., Li, J., Ma, Z., Pan, L., Shi, Y.: MXenes and their applications in wearable sensors. Front. Chem. **8** (2020)
40. Hasan, M.M., Hossain, M.M., Chowdhury, H.K.: Two-dimensional MXene-based flexible nanostructures for functional nanodevices: a review. J. Mater. Chem A **9** (2021)

41. Ma, C., Ma, M.G., Si, C., Ji, X.X., Wan, P.: Flexible MXene-based composites for wearable devices. Adv. Funct. Mater. **31** (2021)
42. Riazi, H., Taghizadeh, G., Soroush, M.: MXene-based nanocomposite sensors. ACS Omega **6**(17) (2021)
43. Chaudhary, V., Gautam, A., Mishra, Y.K., Kaushik, A.: Emerging MXene–polymer hybrid nanocomposites for high-performance ammonia sensing and monitoring. Nanomaterials **11**(10) (2021 Sep. 24)
44. Shi, X., Wang, H., Xie, X., Xue, Q., Zhang, J., Kang, S., et al.: Bioinspired ultrasensitive and stretchable MXene-based strain sensor via nacre-mimetic microscale "brick-and-Mortar" architecture. ACS Nano **13**(1) (2019)
45. Kumar, J.A., Prakash, P., Krithiga, T., Amarnath, D.J., Premkumar, J., Rajamohan, N., et al.: Methods of synthesis, characteristics, and environmental applications of MXene: a comprehensive review. Chemosphere **286** (2022)
46. Mehdi Aghaei, S., Aasi, A., Panchapakesan, B.: Experimental and theoretical advances in MXene-based gas sensors. ACS Omega **6** (2021)
47. Ho, D.H., Choi, Y.Y., Jo, S.B., Myoung, J.M., Cho, J.H.: Sensing with MXenes: progress and prospects. Adv. Mater. (2021)
48. Li, D., Liu, G., Zhang, Q., Qu, M., Fu, Y.Q., Liu, Q., et al.: Virtual sensor array based on MXene for selective detections of VOCs. Sens. Actuators B Chem. **331** (2021)
49. Du, C.F., Zhao, X., Wang, Z., Yu, H., Ye, Q.: Recent advanced on the mxene–organic hybrids: Design, synthesis, and their applications. Nanomaterials **11** (2021)
50. Zhang, W., Ma, C., Huang, L.Z., Guo, W.Y., Li, D.D., Bian, J., et al.: Stretchable, antifreezing, non-drying, and fast-response sensors based on cellulose nanocomposite hydrogels for signal detection. Macromol. Mater. Eng. (2021)
51. Ma, Z., Li, S., Wang, H., Cheng, W., Li, Y., Pan, L., et al.: Advanced electronic skin devices for healthcare applications. J. Mater. Chem. B **7** (2019)
52. Li, Q., Li, Y., Zeng, W.: Preparation and application of 2D MXene-based gas sensors: a review. Chemosensors **9** (2021)
53. Liu, M., Wang, Z., Song, P., Yang, Z., Wang, Q.: Flexible MXene/rGO/CuO hybrid aerogels for high performance acetone sensing at room temperature. Sens. Actuators B Chem. **1**, 340 (2021)
54. Cai, Y., Shen, J., Ge, G., Zhang, Y., Jin, W., Huang, W., et al.: Stretchable $Ti_3C_2T_x$ MXene/carbon nanotube composite based strain sensor with ultrahigh sensitivity and tunable sensing range. ACS Nano **12**(1) (2018)
55. An, H., Habib, T., Shah, S., Gao, H., Radovic, M., Green, M.J., et al.: Surface-agnostic highly stretchable and bendable conductive MXene multilayers. Sci. Adv. **4**(3) (2018)
56. Zhang, Y.Z., Lee, K.H., Anjum, D.H., Sougrat, R., Jiang, Q., Kim, H., et al.: MXenes stretch hydrogel sensor performance to new limits. Sci. Adv. **4**(6) (2018)
57. Gasparini, A.: MXenes materials could be used in wearable pressure sensors. Scilight **2020**(45) (2020)
58. Ma, Y., Liu, N., Li, L., Hu, X., Zou, Z., Wang, J., et al.: A highly flexible and sensitive piezoresistive sensor based on MXene with greatly changed interlayer distances. Nat. Commun. **8**(1) (2017)
59. Yue, Y., Liu, N., Liu, W., Li, M., Ma, Y., Luo, C., et al.: 3D hybrid porous Mxene-sponge network and its application in piezoresistive sensor. Nano Energy **50** (2018)
60. Guo, Y., Zhong, M., Fang, Z., Wan, P., Yu, G.: A wearable transient pressure sensor made with MXene nanosheets for sensitive broad-range human-machine interfacing. Nano Lett. **19**(2) (2019)
61. Ma, Y., Yue, Y., Zhang, H., Cheng, F., Zhao, W., Rao, J., et al.: 3D synergistical MXene/reduced graphene oxide aerogel for a piezoresistive sensor. ACS Nano **12**(4) (2018)
62. Wang, K., Lou, Z., Wang, L., Zhao, L., Zhao, S., Wang, D., et al.: Bioinspired interlocked structure-induced high deformability for two-dimensional titanium carbide (MXene)/natural microcapsule-based flexible pressure sensors. ACS Nano **13**(8) (2019)

63. Chen, X., Sun, X., Xu, W., Pan, G., Zhou, D., Zhu, J., et al.: Ratiometric photoluminescence sensing based on Ti_3C_2 MXene quantum dots as an intracellular pH sensor. Nanoscale **10**(3) (2018)
64. Lei, Y., Zhao, W., Zhang, Y., Jiang, Q., He, J.H., Baeumner, A.J., et al.: A MXene-based wearable biosensor system for high-performance in vitro perspiration analysis. Small **15**(19) (2019)
65. Yang, Y.C., Lin, Y.T., Yu, J., Chang, H.T., Lu, T.Y., Huang, T.Y., et al.: MXene nanosheet-based microneedles for monitoring muscle contraction and electrostimulation treatment. ACS Appl Nano Mater. **4**(8), 7917–7924 (2021)
66. Soomro, R.A., Jawaid, S., Kalawar, N.H., Tunesi, M., Karakuş, S., Kilislioğlu, A., et al.: In-situ engineered MXene-TiO2/BiVO4 hybrid as an efficient photoelectrochemical platform for sensitive detection of soluble CD44 proteins. Biosens Bioelectron. **15**, 166 (2020)
67. Jian, Y., Qu, D., Guo, L., Zhu, Y., Su, C., Feng, H., et al.: The prior rules of designing $Ti_3C_2T_x$ MXene-based gas sensors. Front Chem. Sci. Eng. **15**(3), 505–517 (2021)
68. Dhall, S., Mehta, B.R., Tyagi, A.K., Sood, K.: A review on environmental gas sensors: materials and technologies. Sens. Int. **2** (2021)
69. Ihsanullah, I.: Potential of MXenes in water desalination: current status and perspectives. Nano-Micro Lett. **12** (2020)
70. Sun, Y., Li, Y.: Potential environmental applications of MXenes: a critical review. Chemosphere **271** (2021)
71. Yuan, W., Yang, K., Peng, H., Li, F., Yin, F.: A flexible VOCs sensor based on a 3D Mxene framework with a high sensing performance. J. Mater. Chem. A. **6**(37) (2018)
72. Zhao, L., Wang, K., Wei, W., Wang, L., Han, W.: High-performance flexible sensing devices based on polyaniline/MXene nanocomposites. InfoMat. **1**(3) (2019)
73. Li, X., Xu, J., Jiang, Y., He, Z., Liu, B., Xie, H., et al.: Toward agricultural ammonia volatilization monitoring: a flexible polyaniline/$Ti_3C_2T_x$ hybrid sensitive films based gas sensor. Sens. Actuators B Chem. **316** (2020)
74. Jin, L., Wu, C., Wei, K., He, L., Gao, H., Zhang, H., et al.: Polymeric $Ti_3C_2T_x$ MXene composites for room temperature ammonia sensing. ACS Appl. Nano Mater. **3**(12) (2020)
75. Zhao, L., Zheng, Y., Wang, K., Lv, C., Wei, W., Wang, L., et al.: Highly stable cross-linked cationic polyacrylamide/$Ti_3C_2T_x$ MXene nanocomposites for flexible ammonia-recognition devices. Adv. Mater. Technol. **5**(7) (2020)
76. Yang, Z., Jiang, L., Wang, J., Liu, F., He, J., Liu, A., et al.: Flexible resistive NO2 gas sensor of three-dimensional crumpled MXene $Ti_3C_2T_x$/ZnO spheres for room temperature application. Sens. Actuators B Chem. **326** (2021)
77. Zhu, Z., Liu, C., Jiang, F., Liu, J., Ma, X., Liu, P., et al.: Flexible and lightweight $Ti_3C_2T_x$ MXene@Pd colloidal nanoclusters paper film as novel H_2 sensor. J Hazard Mater. **15**, 399 (2020)
78. Zhang, D., Mi, Q., Wang, D., Li, T.: MXene/Co_3O_4 composite based formaldehyde sensor driven by ZnO/MXene nanowire arrays piezoelectric nanogenerator. Sens. Actuators B Chem. **15**, 339 (2021)
79. Zhang, D., Yu, L., Wang, D., Yang, Y., Mi, Q., Zhang, J.: Multifunctional latex/polytetrafluoroethylene-based triboelectric nanogenerator for self-powered organ-like mxene/metal-organic framework-derived cuo nanohybrid ammonia sensor. ACS Nano **15**(2), 2911–2919 (2021)
80. Li, X., An, Z., Lu, Y., Shan, J., Xing, H., Liu, G., et al.: Room temperature VOCs sensing with termination-modified $Ti_3C_2T_x$ MXene for wearable exhaled breath monitoring. Adv. Mater. Technol. (2021)
81. Sarycheva, A., Polemi, A., Liu, Y., Dandekar, K., Anasori, B., Gogotsi, Y.: 2D titanium carbide (MXene) for wireless communication. Sci. Adv. **4**(9) (2018)
82. Fu, X., Yang, H., Li, Z., Liu, N.C., Lee, P.S., Li, K., et al.: Cation-induced assembly of conductive MXene fibers for wearable heater, wireless communication, and stem cell differentiation. ACS Biomater. Sci. Eng. (2021)

83. Han, M., Liu, Y., Rakhmanov, R., Israel, C., Tajin, M.A.S., Friedman, G., et al.: Solution-processed $Ti_3C_2T_x$ MXene antennas for radio-frequency communication. Adv. Mater. **33**(1) (2021)
84. Li, Y., Tian, X., Gao, S.P., Jing, L., Li, K., Yang, H., et al.: Reversible crumpling of 2D titanium carbide (MXene) nanocoatings for stretchable electromagnetic shielding and wearable wireless communication. Adv. Funct. Mater. **30**(5) (2020)
85. Rasch, F., Postica, V., Schütt, F., Mishra, Y.K., Nia, A.S., Lohe, M.R., et al.: Highly selective and ultra-low power consumption metal oxide based hydrogen gas sensor employing graphene oxide as molecular sieve. Sens. Actuators B Chem. **320** (2020)